A 0.5-Million-Year Record of Millennial-Scale Climate Variability in the North Atlantic

Jerry F. McManus,[1]* Delia W. Oppo[1], James L. Cullen[2]

Long, continuous, marine sediment records from the subpolar North Atlantic document the glacial modulation of regional climate instability throughout the past 0.5 million years. Whenever ice sheet size surpasses a critical threshold indicated by the benthic oxygen isotope ($\delta^{18}O$) value of 3.5 per mil during each of the past five glaciation cycles, indicators of iceberg discharge and sea-surface temperature display dramatically larger amplitudes of millennial-scale variability than when ice sheets are small. Sea-surface temperature oscillations of 1° to 2°C increase in size to approximately 4° to 6°C, and catastrophic iceberg discharges begin alternating repeatedly with brief quiescent intervals. The glacial growth associated with this amplification threshold represents a relatively small departure from the modern ice sheet configuration and sea level. Instability characterizes nearly all observed climate states, with the exception of a limited range of baseline conditions that includes the current Holocene interglacial.

Climatic instability on suborbital time scales (10^3 to 10^4 years) characterized the North Atlantic region during the last glacial period. Rapid oscillations of 5° to 10°C in the atmospheric temperature over Greenland (*1*) and faunal shifts equivalent to more than 4°C in sea-surface temperature (SST) in the subpolar ocean (*2, 3*) occurred repeatedly throughout the 100,000 years following the peak interval of the last interglacial. Millennial-scale pacing of climate variability has continued into the current Holocene interglacial (*4*), but its amplitude has usually been limited to 2° to 3°C over Greenland (*1, 5*) and to less than 2°C in the North Atlantic (*4*), implying that rapid climate change may be amplified during glacial intervals and diminished during interglacial intervals. Records of rapid climate oscillations during previous glacial and interglacial intervals of varying intensity may help to establish whether such a link exists between ice sheet size and regional and global climate instability. We present continuous high-resolution climate records from deep-sea sediments encompassing the last 0.5 million years (My) in the subpolar North Atlantic. These records cover a wide range of global ice volume, from somewhat less than the modern total of 80 m sea-level equivalent to well over 200 m sea-level equivalent and indicate that climatic stability on millennial time scales prevails only when the extent of global glaciation falls within a narrow range, including that of the current Holocene interglacial. Climatic instability is more typical, occurring during fully developed glacials, transitional intervals of ice-sheet growth and decay, and even during stadial portions of interglacials, when limited ice-sheet growth occurs. The threshold separating stable and unstable climatic regimes represents a relatively small departure from the modern ice sheet configuration, whereas sufficiently extreme glaciations may also establish less variable climate states.

The sediments for this study were recovered at Site 980 (Fig. 1) on the Feni abyssal drift during Leg 162 of the Ocean Drilling Program (ODP). Previous studies of the last climate cycle (*2, 6*) confirmed that regional climate variations are faithfully recorded in the rapidly accumulating sediments on Feni (13 cm/ky in the sediments studied here). A chronostratigraphy for Site 980 was established using the oxygen isotope ratio ($\delta^{18}O$) of calcite shells secreted by the protozoan *Cibicidoides wuellerstorfi*, an epifaunal benthic (bottom-dwelling) foraminifera (Fig. 2). The conventional glacial (even) and interglacial (odd) marine isotope stages (MIS) (*7*) were easily identified in the benthic $\delta^{18}O$ record, and an orbitally tuned age model was derived by graphical correlation with existing deep-sea chronologies (*8*). The 65-m section we examined represents 0.5 My of deposition and captures five of the large-amplitude glacial-interglacial (G-IG) cycles of ~100-ky duration that have characterized the global climate record during this time.

We examined two proxies of sea-surface conditions: the relative abundance of ice-rafted debris (IRD), and the $\delta^{18}O$ of the planktic (surface-dwelling) foraminifera *Neogloboquadrina pachyderma*, dextral-coiling (*N. pachyderma d.*). The glacial occurrence of IRD throughout much of the region is long-established (*9*), and episodic pulses of IRD (*10, 11*) were among the first clues for suborbital variability in the glacial North Atlantic. Planktic foraminiferal $\delta^{18}O$ is influenced by the temperature and $\delta^{18}O$ of ambient seawater (*7*), and is therefore a useful indicator of sea-surface hydrography. We also examined benthic $\delta^{13}C$, a proxy for changes in deep ocean circulation.

Ice-rafting at Site 980 (Fig. 2) is episodic throughout, with repeated peaks of IRD concentrations surpassing 500 lithics per gram. None of these peaks lasts for more than a few thousand years, and the abundance always returns to very low baseline values before rising again, even during times of large continental ice sheets. The size and frequency of the IRD events increases, however, along with the size of the ice sheets during each 100-ky cycle. Within the youngest portion of the Site 980 record, the largest peaks include the well-documented "Heinrich events," catastrophic iceberg discharges that punctuated the last glacial (*10, 11*). More than 50 comparable IRD peaks occur throughout the entire record, indicating that such episodic behavior is a fundamental aspect of Pleistocene glacial cycles. Ice-rafting is generally diminished during interglacials. This is most likely related to the simple requirement of sufficient continental ice near the North Atlantic prior to catastrophic discharge, although even the modest ice growth within stadial substages of MIS 5, 7, and 9, the last three interglacials, has associated IRD events. The concentration of the largest IRD peaks within the glacial half of each 100-ky cycle yields a repeat time of approximately 6 ky (40 events in 250 ky). Although this might suggest that a lower frequency of recurrence prevails during interglacial intervals, it is also possible that the frequency of the events themselves remains the same (*4*), and that amplitude modulation

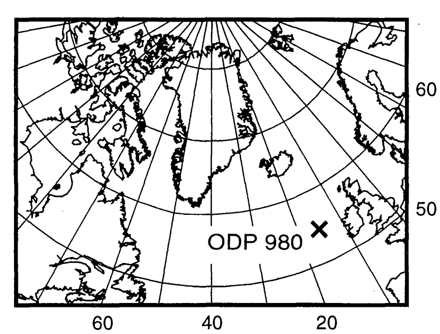

Fig. 1. Location of ODP Site 980 (55°29′N, 14°42′W, depth of 2179 m) in the eastern North Atlantic.

[1]Woods Hole Oceanographic Institution, Woods Hole, MA 02543, USA. [2]Salem State College, Salem, MA 01970, USA.

*To whom correspondence should be addressed. E-mail: jmcmanus@whoi.edu

renders the size of the events more prominent, and thus easily identifiable, during glacial intervals.

The relationship between benthic $\delta^{18}O$ and both the initial and final IRD pulses of each 100-ky cycle is noteworthy. During each cycle, an IRD event follows the first increase in benthic $\delta^{18}O$ to values exceeding 3.5 per mil. Likewise, a large IRD event accompanies each of the rapid deglaciations, or "terminations" (*12*), from values greater than 4.0 per mil, through 3.5 per mil, to less than 3.0 per mil. The close association of the onset and cessation of ice-rafting events with a particular value in the benthic $\delta^{18}O$ proxy for ice volume suggests that this value represents an important threshold in ice sheet growth.

Neogloboquadrina pachyderma d. is abundant in subpolar regions and constitutes >10% of the coretop fossil assemblage underlying nearly all North Atlantic surface waters with summer SST of 10° to 20°C (*13*). Despite the dramatic and repeated changes in the planktic foraminiferal assemblage that occurred near Site 980 during the last 0.5 My (*14*), *N. pachyderma d.* was present throughout, yielding a continuous $\delta^{18}O$ record (Fig. 2) containing several large-amplitude (3.0 per mil) 100-ky G-IG cycles. Rapid 1.0–per mil oscillations occur within the glacial portion of each large cycle, while variability is limited to 0.1 to 0.3 per mil during peak interglacials.

Previous studies indicate that *N. pachyderma d.* $\delta^{18}O$ is useful as a proxy for SST during the Late Pleistocene in the subpolar North Atlantic (*15*). Before considering the climatic implications of the Site 980 *N. pachyderma d.* $\delta^{18}O$ record, we therefore converted the values to estimates of SST by removing the global signature of ice volume, as captured by the normalized benthic *C. wuellerstorfi* $\delta^{18}O$ (*16*). The resulting isotopic paleothermometer has several distinct benefits for assessing variability throughout the record. First, the large dynamic range is not subject to signal saturation at warm or cold extremes, which might limit other methods, such as those based on faunal percentages. Second, the $\delta^{18}O$-temperature relationship (*7, 17*) allows a direct comparison of the amplitude of climate changes at different times in the past. Third, any diminished interglacial variability at Site 980 is unlikely to be a result of faunal saturation through seasonal or depth migration of the foraminifera, because peak SSTs are well within the range tolerated by *N. pachyderma d.* in the modern ocean (*13*).

The temperature estimates (Fig. 3) confirm that SST varied throughout the last 0.5 My, reaching 13° to 15°C during each interglacial and falling to 5° to 7°C within each glacial. During each G-IG cycle, ΔSST was 8° to 9°C, comparable to faunally derived estimates (*18*) from studies of each of the last two G-IG cycles near Site 980. Although the SST minima, maxima, and therefore the overall ΔSST are all in close agreement with previous estimates, the character of the Site 980 record is distinctive. Each of the glacial intervals is interrupted repeatedly by rapid 3° to 6°C oscillations. Only within MIS 12 (and possibly MIS 2) is there any extended glacial interval with SST variability of less than 4°C. Interglacial SSTs are generally less variable, although excursions of 3° to 5°C occur within stadial substages of MIS 5 and MIS 9.

The Site 980 records confirm the fundamentally dynamic nature of the Pleistocene ice ages. Harsh conditions prevailed repeatedly in the North Atlantic, yet never for more than a few

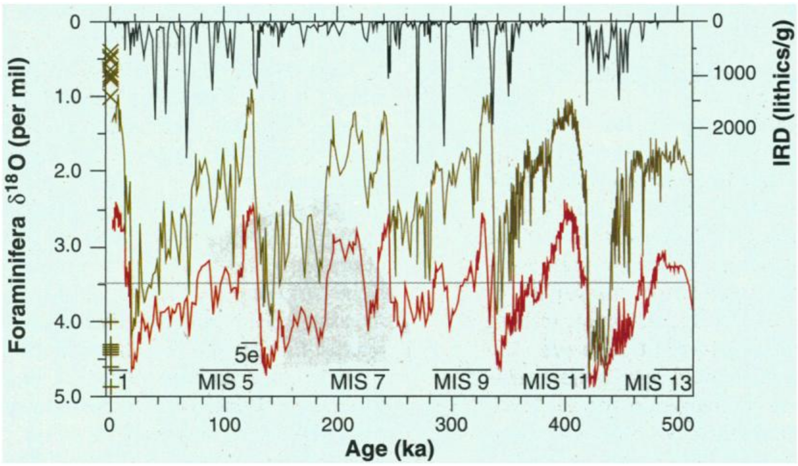

Fig. 2. Time series of IRD and isotopic measurements from Site 980 (sample resolution varies from 300 to 1200 years). IRD is plotted as the number of detrital sediment grains (lithics), larger than 150 μm, per bulk sample weight. Benthic (*C. wuellerstorfi*, red) and planktic (*N. pachyderma d.*, green) foraminifera $\delta^{18}O$ values are plotted relative to the Pee Dee belemnite (*Belemnitella*) (PDB) standard (*7*). Isotope measurements were made at the Woods Hole Oceanographic Institution on a Finnigan MAT252 coupled to an automated carbonate preparation device consisting of 46 single-reaction chambers, with 23 chambers on each of two lines. Acid temperature was ~70°C. The standard deviation of the isotope values of National Bureau of Standards (NBS) carbonate standard NBS19 is 0.08 per mil and 0.04 per mil for $\delta^{18}O$ and $\delta^{13}C$, respectively. Calibration to PDB was via NBS19 ($\delta^{18}O$ = –2.2 VPDB, $\delta^{13}C$ = 1.95 VPDB). Data points at 0 ky are $\delta^{18}O$ measurements on modern *N. pachyderma d.* from Atlantic sediment traps at 47°N (×) and 65°N (+), demonstrating an isotopic range surpassing that of our sedimentary data. The modern data from 65°N are adjusted by 1.0 per mil, a minimum estimate of past mean ocean changes (*28*), for comparison to glacial data. Interglacial MIS and the last peak interglacial substage 5e are indicated for reference.

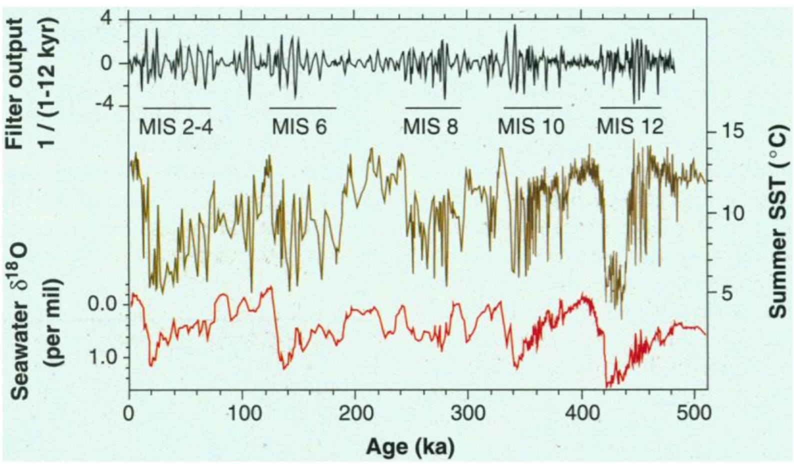

Fig. 3. Time series of SST and seawater $\delta^{18}O$ from Site 980. Seawater $\delta^{18}O$, the ice volume component of benthic $\delta^{18}O$, was obtained by adjusting benthic $\delta^{18}O$ for a 3°C interglacial warming of the deep ocean. SST was calculated by subtracting changes in the ice volume signal from planktic $\delta^{18}O$ and scaling the isotopic residual as a departure from modern temperature (*15*). The scaling factor varies from –0.21 to –0.23 per mil/°C, in accord with a paleotemperature equation, $T = 15.18 - 4.79(\delta c - \delta w) + 0.08(\delta c - \delta w)^2$, derived from recent measurements (*17*) of the equilibrium oxygen isotopic fractionation ($\delta^{18}O$) between calcite (δc) and water (δw). Filter output results are derived from interpolation of SST data at 500-year increments and application of a zero phase, 128-order, Hamming window with cutoff frequencies of 1/1 and 1/12 ky. Glacial MIS are indicated for reference.

thousand years. Variability on millennial time scales has thus been the rule, rather than the exception. This characteristic may help explain the current failure of coupled ocean-atmosphere global climate models to achieve a stable equilibrium glacial climate. As indicated by benthic $\delta^{18}O$, ice volume was instrumental in setting the degree of climate stability. No large oscillations occur when the benthic $\delta^{18}O$ is at minimum values and few occur when it is less than 3.5 per mil (Fig. 2). The longest relatively ice-free interval occurred during interglacial MIS 11, which also has the longest interval (30 to 40 ky) without amplified millennial-scale SST (and IRD) variability. MIS 11 has long been held to be an especially mild interglacial in many respects (*19*), and such a particularly IRD-free interval may indicate diminished calving or size of the Greenland ice sheet, or both, in addition to the absence of other circum–North Atlantic ice sheets. Briefer intervals of relative climate stability occurred during the portions of MIS 5, 7, 9, and 13 with the least ice volume. During these peak interglacials, SST variations were limited to 1° to 2°C. Following the last crossing of the 3.5–per mil threshold, at the time of the Younger Dryas climatic reversal, diminished amplitudes also characterized the variability in MIS 1 (*4, 5*). Such times of diminished ice volume appear to be respites from the prevailing instability of the last 0.5 My.

The persistence of climatic variability is unequivocal, but its cause remains obscure. The millennial time scale of the observed changes, the apparently heightened sensitivity of the North Atlantic region (*20*), and the theoretical existence of multiple quasi-stable modes (*21*), all suggest that changes in the ocean's thermohaline circulation (*22, 23*) may play a role. In order to assess this possibility, we have also evaluated the relative vigor of the northern component of the deep circulation by examining the carbon isotopic ratio ($\delta^{13}C$) of *C. wuellerstorfi* at Site 980. Although multiple factors may affect the $\delta^{13}C$ of benthic calcite, to first approximation, the signal at Site 980 can be attributed to the varying influence of competing water masses below 2 km water depth in the subpolar North Atlantic (*22, 23*). Northern source water (North Atlantic deep water, or NADW, and glacial North Atlantic intermediate water, or GNAIW) is nutrient-depleted, with high $\delta^{13}C$ values, and southern source water is nutrient-rich, with low $\delta^{13}C$ values. Throughout the last 0.5 My, the benthic $\delta^{13}C$ at Site 980 has varied repeatedly (Fig. 4) on similar time scales as the SST and IRD signals, with stronger influence of northern source water associated with warmer temperatures and minimal ice-rafting. It is tempting to link these observations, considering the poleward heat transport associated with vigorous deepwater production; however, variability in the $\delta^{13}C$ signal continues throughout the record, without a threshold at the 3.5– per mil benthic $\delta^{18}O$ value. Significant oscillations (>0.4 per mil) occur even during the peak interglacials at MIS 1, 5e, and 11, when benthic $\delta^{18}O$ dropped to 2.5 per mil, SST variations were minimal, and IRD input was negligible. The persistence of variability during relatively ice-free intervals makes it unlikely that the oscillations in thermohaline circulation are driven by temperature or salinity perturbations associated with catastrophic iceberg discharge events. It is more likely that each diminuition of NADW production and associated poleward oceanic heat transport, whether caused by ocean-atmosphere interactions or internal oscillations, contributes to lowered SST and increased ice-rafting. When ice sheets are of sufficient size to produce abundant icebergs, their meltwater would then serve as a positive feedback, stabilizing the upper water column and further diminishing NADW (*6, 10, 11*). This interpretation is supported by the fact that many of the $\delta^{13}C$ minima associated with the largest IRD events are particularly prominent, including those that accompany each glacial termination. The lack of a clear correspondence between subtle SST changes and $\delta^{13}C$ during peak interglacials may indicate the limited influence of circulation changes on SST in the absence of such feedbacks.

Site 980 is at a sensitive depth to monitor changes in the thermohaline circulation because it is bathed by deep water just below the hinge line of glacial partitioning of the water column (*23*). The proximity to this important boundary also lends caution to our interpretation of the benthic $\delta^{13}C$. Small shifts in water masses across a steep gradient may be recorded as large amplitude changes in physical and chemical properties at a single location. The interpretation of the $\delta^{13}C$ record will need to be refined as comparable high-resolution records at additional depths and locations become available. Nevertheless, Site 980 appears to capture persistent, significant variability in the deep circulation. The largest interglacial (>0.4 per mil) and glacial (>1.0 per mil) amplitudes are comparable to the entire range of values found in the modern (*24*) and glacial (*22, 23*) North Atlantic. Many smaller amplitude oscillations occur as well, suggesting that the Site 980 $\delta^{13}C$ record does not exhibit a square wave alternation between the characteristic values of two different water masses, but rather approximates the relative influence of those water masses at the site, as set by the basin-wide state of circulation.

The occurrence of circulation changes during interglacial intervals suggests that neither a glacial salt-oscillator (*25*) nor a binge-purge iceberg discharge mechanism (*26*) can fully account for the persistent variability. One alternative, an extension of the oscillator concept (*22*), may be that the thermohaline circulation does not operate at an equilibrium level of salt and freshwater transport, but alternates between modes that export an excess of one or the other. Such an oscillator would operate regardless of glacial state, while remaining sensitive to the same glacial influence that is evident in the surface climate proxies.

That the presence and size of ice sheets should influence climate is not surprising, given their affect on the atmospheric circulation and hydrologic balance (*27*). It is nonetheless instructive to note the small ice volume change associated with the onset of a dramatic shift in the climate response. A rise in benthic $\delta^{18}O$ from the peak interglacial minimum of 2.5 per mil to the 3.5 per mil level constitutes half of the range for each 100-ky G-IG cycle, yet it represents proportionately little growth in ice or fall in sea level, because much of the $\delta^{18}O$ rise

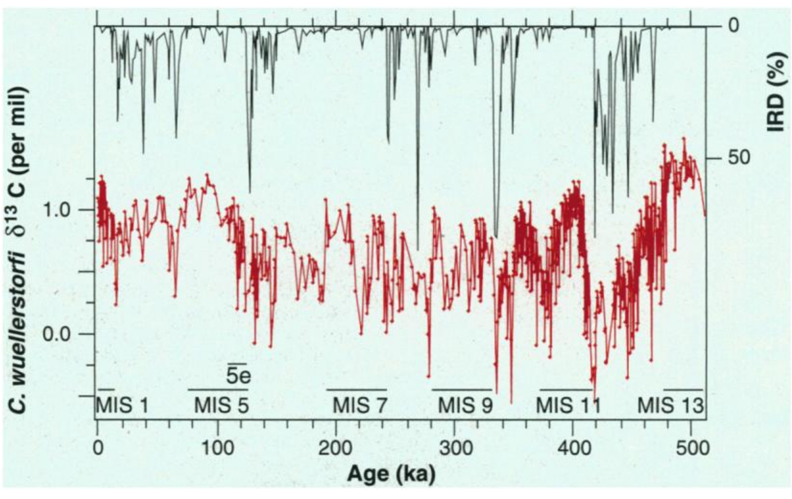

Fig. 4. Time series of IRD and benthic carbon isotopic ($\delta^{13}C$, per mil) measurements from Site 980. IRD is plotted as the percentage of sediment grains larger than 150 μm that are detrital. This particular IRD index is not sensitive to changes in mean sedimentation rate, which may be influenced by variations in abyssal currents associated with the strength of thermohaline circulation. Benthic $\delta^{13}C$ values are plotted relative to the PDB standard. Interglacial MIS and the last peak interglacial substage 5e are indicated for reference.

over that interval reflects cooling of the deep ocean (*28, 29*). The 3.5–per mil threshold thus corresponds to glacial ice growth that lowers sea level as little as 30 m below the modern (2.5 per mil) level. Although this change is not negligible, it represents no more than 25% of the total 120-m difference between modern sea level and that of the last glacial maximum (*28*). It is also significantly less than the existing 80-m sea level depression which is due to modern ice volume (*30*).

The sharp contrast in variability at benthic $\delta^{18}O$ values above and below approximately 3.5 per mil suggests that the extent of glaciation corresponding to this value constitutes an important and persistent physical threshold. Indeed, a similar relationship between benthic $\delta^{18}O$ and IRD events was documented between 1.2 and 1.4 million years ago (*31*), and major ice-rafting in the subpolar North Atlantic did not begin prior to the attainment of comparable benthic $\delta^{18}O$ values 2.5 to 2.7 million years ago (*32*).

Although the physical significance of the 3.5–per mil threshold is difficult to establish, there are several possibilities. It represents a total amount of global ice (approximately equivalent to 105 to 110 m of sea level), which may itself be important, as the distribution of water between solid and liquid phase has implications for the hydrologic cycle. Alternatively, the location of ice may be the crucial factor, influenced in turn by the amount. The 3.5–per mil threshold may represent ice growth across a key strait such as North Greenland–Canada, or the establishment of grounding and export of ice from marginal-sea nucleation sites (*33*). The key factor may be sea ice advance associated with glacial ice growth. Extensive sea ice growth in the Labrador and Nordic seas, and in the North Atlantic, would all increase the regional sensitivity to changes in ocean heat transport. Yet another possibility is the importance of the shape and height of ice sheets. The growing Laurentide ice sheet would eventually interact with the jet stream, deflecting it southward and cooling the North Atlantic (*27*). The associated steepening of meridional SST gradients would also sensitize the subpolar North Atlantic to variations in poleward ocean heat transport. Although such a steepening of gradients has almost certainly occurred (*14, 18*), it is less well established whether this was due to a particular ice sheet size or geometry. The 3.5–per mil threshold may also result from a combination of the factors mentioned here.

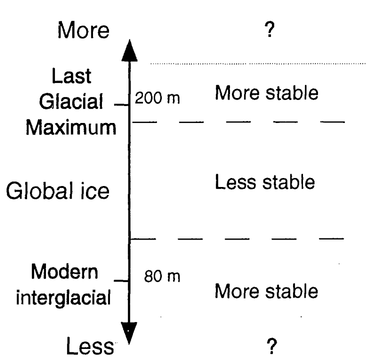

Fig. 5. Schematic representation of possible climatic stability regimes.

The possibility of another, less dramatic threshold at larger ice volumes is suggested by the relative diminuition of SST variability during MIS 12, the most severe glaciation of the last 0.5 My (*29*). As was previously documented in the North Atlantic region (*1, 2*), variability at Site 980 was also diminished during MIS 2, although not in the comparable MIS 6, so these glaciations of 4.5 to 4.6 per mil in benthic $\delta^{18}O$ may just achieve a second, glacial, threshold. The evidence from MIS 12 suggests that sufficiently large ice sheets might be associated with climate regimes of diminished variability. It is also possible that the peak interglacial and glacial intervals of the past 0.5 My are not climatic end members, but lie within zones of relative stability, beyond which variability might increase again (Fig. 5). This possibility is supported by model results predicting enhanced instability due to changes in the hydrologic cycle associated with both warmer (*34*) and colder (*35*) departures from modern interglacial conditions. Because the range of climate states examined in this study covers nearly the entire range of those found in the Quaternary, subsequent attempts to evaluate this possibility may need to reach farther back in the geologic record, or rely at least partially on mathematical models.

References and Notes

1. W. Dansgaard and H. Oeschger, in *The Environmental Record in Glaciers and Ice Sheets*, H. Oeschger and C. C. Langway, Eds. (Wiley, Chichester, UK, 1989), pp. 287–318; S. J. Johnsen *et al.*, *Nature* **359**, 311 (1992); P. M. Grootes, M. Stuiver, J. W. C. White, S. Johnsen, J. Jouzel, *ibid.* **366**, 552 (1993).
2. G. C. Bond *et al.*, *Nature* **365**, 143 (1993); J. F. McManus *et al.*, *ibid.* **371**, 326 (1994).
3. D. W. Oppo, M. Horowitz, S. J. Lehman, *Paleoceanography* **12**, 51 (1997).
4. A. McIntyre and B. Molfino, *Science*, **274**, 1867 (1996); L. D. Keigwin, *ibid.*, p. 1504; G. C. Bond *et al.*, *ibid.* **278**, 1257 (1997); P. A. Mayewski *et al.*, *J. Geophys. Res.* **102**, 345 (1997).
5. R. B. Alley *et al.*, *Geology* **25**, 483 (1997).
6. L. Labeyrie *et al.*, *Philos. Trans. R. Soc. London Ser. B* **348**, 255 (1995).
7. C. Emiliani, *J. Geol.* **63**, 539 (1955).
8. D. G. Martinson *et al.*, *Quat. Res.* **27**, 1 (1987); N. J. Shackleton, A. Berger, W. R. Peltier, *Trans. R. Soc. Edinburgh Earth Sci.* **81**, 251 (1990).
9. M. N. Bramlette and W. H. Bradley, *USGS Prof. Pap. 196-A* (1941); W. F. Ruddiman, *Geol. Soc. Am. Bull.* **88**, 1813 (1977).
10. H. Heinrich, *Quat. Res.* **29**, 143 (1988); G. C. Bond *et al.*, *Nature* **360**, 245 (1992); W. S. Broecker, G. C. Bond, M. Klas, E. Clark, J. F. McManus, *Clim. Dyn.* **6**, 265 (1992); F. E. Grousset *et al.*, *Paleoceanography* **8**, 175 (1993); S. A. van Kreveld, M. Knappertsbusch, J. Ottens, G. Ganssen, J. E. van Hinte, *Mar. Geol.* **131**, 21 (1996).
11. J. F. McManus, R. F. Anderson, W. S. Broecker, M. Q. Fleisher, S. M. Higgins, *Earth Planet. Sci. Lett.* **135**, 29 (1998).
12. W. S. Broecker and J. van Donk, *Rev. Geophys. Space Phys.* **8**, 169 (1970); W. Broecker, in *Milankovitch and Climate, Part 2*, A. Berger *et al.*, Eds. (Reidel, Norwell, MA, 1984), pp. 687–698.
13. A. W. H. Be and D. S. Tolderlund, in *Micropaleontology of Oceans*, B. M. Funnell and W. R. Riedel, Eds. (Cambridge Univ. Press, London, 1971), pp. 105–147; N. G. Kipp, *Geol. Soc. Am. Mem.* **145**, 3 (1976); U. Pflaumann, J. Duprat, C. Pujol, L. D. Labeyrie, *Paleoceanography* **11**, 15 (1996).
14. W. F. Ruddiman and A. McIntyre, *Geol. Soc. Am. Mem.* **145**, 3 (1976).
15. Several factors may influence planktic $\delta^{18}O$. Independent estimates of the G-IG contrast in SST (8° to 10°C) based on changes in planktic faunal assemblages in the subpolar North Atlantic (*18, 36*), when combined with the 1.0 to 1.3 per mil change in mean ocean $\delta^{18}O$ due to changes in ice volume (*28, 29*), would predict a planktic $\delta^{18}O$ amplitude of approximately 3 per mil. Many foraminifera species do not persist through such SST changes, or display diminished isotopic amplitudes [J. C. Duplessy *et al.*, *Oceanol. Acta* **14**, 311 (1991)], but previous studies [(*3, 11, 36*); L. D. Keigwin and G. A. Jones, *Deep-Sea Res.* **36**, 845 (1989)] indicate that the $\delta^{18}O$ of *N. pachyderma d.* captures nearly the full SST range, approaching and even exceeding 3 per mil. The close agreement between the observed isotopic temperature estimates and those predicted by faunal assemblages leaves little room for significant contributions to the observed *N. pachyderma d.* $\delta^{18}O$ by changes in local salinity or the dissolved carbonate ion concentration [H. J. Spero, J. Bijma, D. W. Lea, B. E. Bemis, *Nature* **390**, 497 (1997)], except as they might cancel each other due to opposite sign. Therefore, we conclude that the primary influence on the Site 980 *N. pachyderma d.* $\delta^{18}O$ record is SST, with a secondary influence of global ice volume. On shorter time scales, when ice volume changes are negligible, ΔSST estimates derived from *N. pachyderma d.* $\delta^{18}O$ and those implied by faunal assemblages have also been shown to be in close agreement (*36*), with no additional adjustment required. This fidelity may result in part from the broad temperature tolerance of this species. After an ice-volume adjustment, measurements of *N. pachyderma d.* $\delta^{18}O$ in the modern ocean (Fig. 2) yield an even wider range of values than found in the Site 980 sediments.
16. Benthic $\delta^{18}O$ is primarily determined by ice volume, but is also affected by the temperature of the deep ocean. The best estimates (*28, 29*) for this effect during the last large climate cycle indicate that most of the temperature change is associated with MISs 1 and 5e, and by extension, the onset and demise of all peak interglacials. After a 0.7–per mil adjustment for this 3°C temperature effect in each 100-ky cycle, the remaining seawater component of benthic $\delta^{18}O$ was removed from the *N. pachyderma d.* $\delta^{18}O$.
17. S.-T. Kim and J. R. O'Neil, *Geochim. Cosmochim. Acta* **61**, 3461 (1997).
18. CLIMAP Project Members, *Science* **191**, 1131 (1976); J. C. Duplessy, L. D. Labeyrie, M. Paterne, in *Late Quaternary Paleoceanography of the North Atlantic Margins*, J. T. Andrews, W. E. N. Austin, H. Bergsten, A. E. Jennings, Eds. (The Geological Society Publishing House, Bath, UK, 1996), pp. 167–175; E. Cortijo *et al.*, *Nature* **372**, 446 (1994).
19. L. H. Burckle, *Quat. Sci. Rev.* **12**, 825 (1993); D. A. Hodell, *Paleoceanography* **8**, 47 (1993); W. R. Howard, *Nature* **388**, 418 (1997).
20. W. S. Broecker, D. M. Peteet, D. Rind, *Nature* **315**, 21 (1985); H. Oeschger *et al.*, in *Climate Processes and Climate Sensitivity*, J. E. Hansen and T. Takahashi, Eds. (American Geophysical Union, Washington, DC, 1984), vol. 5, pp. 299–306.
21. S. Manabe and R. J. Stouffer, *J. Clim.* **1**, 841 (1988).
22. E. A. Boyle and L. Keigwin, *Nature* **330**, 35 (1987); D. W. Oppo and R. G. Fairbanks, *Earth Planet. Sci. Lett.* **86**, 1 (1987); J. C. Duplessy *et al.*, *Paleoceanography* **3**, 343 (1988).
23. D. W. Oppo and S. J. Lehman, *Science* **259**, 1148 (1993).
24. P. Kroopnick, *Earth Planet. Sci. Lett.* **49**, 469 (1980).
25. W. S. Broecker, G. Bond, M. Klas, G. Bonani, W. Wolfli, *Paleoceanography* **5**, 469 (1990).
26. D. R. MacAyeal, *ibid.* **8**, 775 (1993).
27. S. Manabe and A. J. Broccoli, *J. Geophys. Res.* **90**, 2167 (1985).
28. J. Chappell and N. J. Shackleton, *Nature* **324**, 137

(1986); L. Labeyrie, J.-C. Duplessy, P. L. Blanc, *ibid.* **327**, 477 (1987); R. G. Fairbanks, *ibid.* **342**, 637 (1989); D. P. Schrag, G. Hampt, D. W. Murray, *Science* **272**, 1930 (1996).
29. N. J. Shackleton, *Quat. Sci. Rev.* **6**, 183 (1987).
30. A. Baumgartner and E. Reichel, *The World Water Balance* (Elsevier, New York, 1975), pp. 1–179; R. S. Williams Jr. and D. K. Hall, in *Atlas of Earth Observations Related to Global Change*, R. J. Gurney, J. L. Foster, C. L. Parkinson, Eds. (Cambridge Univ. Press, Cambridge, 1993), pp. 401–422.
31. M. E. Raymo, K. Ganley, S. Carter, D. W. Oppo, J. McManus, *Nature* **392**, 699 (1998).
32. N. J. Shackleton *et al.*, *ibid.* **307**, 420 (1984).
33. G. H. Denton and T. J. Hughes, in *The Last Great Ice Sheets*, G. H. Denton and T. J. Hughes, Eds. (Wiley, New York, 1981), pp. 440–467.
34. A. J. Weaver and T. M. C. Hughes, *Nature* **367**, 447 (1994).
35. K. Sakai and W. R. Peltier, *J. Clim.* **10**, 949 (1996).
36. D. W. Oppo, J. F. McManus, J. L. Cullen, *Science* **279**, 1335 (1998).
37. L. Zou, T. Norris, S. Healey, D. Ostermann, and M. Jeglinski provided invaluable technical assistance. W. Curry and D. Ostermann generously shared unpublished data from the Iceland Plateau and sediment trap samples from the North Atlantic. Comments from W. Curry and T. Marchitto improved the manuscript. Supported by NSF, U.S. Science Support Program, and a Woods Hole Oceanographic Institution postdoctoral scholarship.

5 October 1998; accepted 6 January 1999

A Kuroko-Type Polymetallic Sulfide Deposit in a Submarine Silicic Caldera

K. Iizasa,[1] R. S. Fiske,[2*] O. Ishizuka,[1] M. Yuasa,[1] J. Hashimoto,[3] J. Ishibashi,[4] J. Naka,[3] Y. Horii,[5] Y. Fujiwara,[3] A. Imai,[4] S. Koyama[3]

Manned submersible studies have delineated a large and actively growing Kuroko-type volcanogenic massive sulfide deposit 400 kilometers south of Tokyo in Myojin Knoll submarine caldera. The sulfide body is located on the caldera floor at a depth of 1210 to 1360 meters, has an area of 400 by 400 by 30 meters, and is notably rich in gold and silver. The discovery of a large Kuroko-type polymetallic sulfide deposit in this arc-front caldera raises the possibility that the numerous unexplored submarine silicic calderas elsewhere might have similar deposits.

Kuroko-type polymetallic sulfide deposits, as described from the Miocene rocks of the Hokuroku district in northern Honshu, Japan, are formed on the sea floor and genetically related to silicic submarine volcanoes (*1*). Heat from magma reservoirs beneath these volcanoes forms convecting hydrothermal systems that leach heavy metals from shallow crustal rocks. As they rise through fissures or volcanic conduits, hot aqueous fluids carry these metals to the sea floor, where they precipitate polymetallic sulfide deposits as they encounter cold seawater. Kuroko-type deposits in ancient rock sequences are important sources of Cu, Zn, Pb, Ag, and Au that have been exploited economically in many countries (*2, 3*).

Here, we describe a major Kuroko-type deposit in Myojin Knoll Caldera, which is located 400 km south of Tokyo (Fig. 1). This is one of nine Quaternary submarine silicic calderas lying on the front of the Izu-Ogasawara Arc (*4*). The caldera rim, 520 to 880 m below sea level, is about 7 km in diameter; its floor is 4 by 3 km and it ranges in depth from 1350 to 1400 m. The caldera's collapse volume is about 18 km^3. The age of the caldera is not yet known. The steep caldera wall exposes a variety of unaltered deposits, including rhyolite lava flows and domes, breccias, and thick sequences of bedded and nonbedded pumice containing 71 to 74 weight % SiO_2 and <1 weight % K_2O. A postcaldera rhyolite dome rises 300 m above the caldera floor (*5*).

Box and gravity cores collected in 1986–1989 provided the first indication of hydrothermal sulfide mineralization (*6*). Anomalous concentrations of methane (to 11 nmol/kg) and manganese (to 170 nmol/kg) in the water column about 300 m above the caldera floor implied that hydrothermal fluids were being emitted locally (*7*). A manned submersible program, begun in 1991, has so far involved 23 dives into the caldera.

The deposit extends from the flat caldera floor at 1360 m to a depth of about 1210 m on the sloping talus at the foot of the eastern caldera wall (Fig. 2). The deposit lies above the interpreted trace of the caldera boundary fault, and its underlying hydrothermal system is probably contained largely within the debris-filled caldera collapse conduit. The caldera-related magma reservoir at depth provides the heat that drives the system, and the collapse conduit connecting this reservoir with the caldera provides a pathway for ascending hydrothermal fluids. The deposit bears no obvious relationship to the postcaldera rhyolite dome, whose center lies more than 2 km to the west.

The exposed part of the sulfide mass, which we call the Sunrise deposit, is at least 400 by 400 m in plan view. Submersible-based sounding profiles along the 1350-m contour and three traverses crossing this contour (Fig. 2) indicate that it rises an average

Table 1. Selected minerals identified in the Sunrise deposit.

	Active chimneys	Inactive chimneys	Mounds, massive and layered	Disseminated in tuff breccia
Anhydrite	*			
Barite	*	*	*	*
Cerussite		*		
Chalcopyrite	*,†	*,†	*	*
Covellite		*	*	*
Galena	*,†	*,†	*	*
Jordanite	*	*		
Marcasite	*	*	*	*
Native arsenic	*			
Native sulfur	*			
Orpiment	*			
Pearceite				*
Pyrargyrite				*
Pyrite	*,‡	*,‡	*,‡	*,†,‡
Realgar	*			
Sphalerite	*,§,‖	*,§,‖	*	*
Tennantite	*	*	*	*
Tetrahedrite	*	*	*	*
Wurtzite	*			

*Present in euhedral to anhedral forms. †Colloform. ‡Pelletal. §Columnar. ‖Dendritic.

[1]Geological Survey of Japan 1-3, Higashi-1, Tsukuba, Ibaraki 305-8567, Japan. [2]Smithsonian Institution MRC-119, Washington, DC 20560–0119, USA. [3]Japan Marine Science & Technology Center 2-15, Natsushima-cho, Yokosuka 237-0061, Japan. [4]University of Tokyo 3-1, Hongo-7, Tokyo 133-0033, Japan. [5]Tokyo Metropolitan Fisheries Station, 4222 Mitsune, Hachijojima, Tokyo 100-1511, Japan.

*To whom correspondence should be addressed. E-mail: rfiske@volcano.si.edu